

**UCLA**

**UCLA Electronic Theses and Dissertations**

**Title**

Establishing Capacity and Demand Factors for Force-Controlled Components in a Rocking Spine System for Reinforced Concrete Frames with Infills Using a Reliability-Based Method

**Permalink**

<https://escholarship.org/uc/item/7d41b1qk>

**Author**

Kusumayani, Ni Made Novia

**Publication Date**

2017

Peer reviewed|Thesis/dissertation

UNIVERSITY OF CALIFORNIA

Los Angeles

Establishing Capacity and Demand Factors for Force-Controlled Components in a  
Rocking Spine System for Reinforced Concrete Frames with Infills Using a Reliability-  
Based Method

A thesis submitted in partial satisfaction  
of the requirements for the degree Master of Science  
in Civil Engineering

by

Ni Made Novia Kusumayani

2017

© Copyright by  
Ni Made Novia Kusumayani

2017

## ABSTRACT OF THE THESIS

Establishing Capacity and Demand Factors for Force-Controlled Components in a Rocking Spine System for Reinforced Concrete Frames with Infills Using a Reliability-Based Method

by

Ni Made Novia Kusumayani

Master of Science in Civil Engineering

University of California, Los Angeles, 2017

Professor Henry J. Burton, Chair

A reinforced concrete frame with rocking spine system is evaluated using reliability-index method with main objective of establishing the load and resistance factors for the force-controlled components. A nonlinear structural model of a six-bay six-story concrete frame building with stiff infill panels idealized as compression only struts was constructed in OpenSees. Spine-infills, spine-beams, and spine-columns, are considered as force-controlled components, while non-spine infills and adjacent beams are considered as deformation-controlled components. The model is evaluated with 44 ground motions through Incremental Dynamic Analysis (IDA) to determine the demands in the force-

controlled components. The model was also evaluated through response spectrum analysis to define the system's yield modification factor,  $R_{\mu}$ , which is used along with hazard curve to obtain the reliability index of the system,  $\beta_{R,H\alpha}$ . The capacity,  $\phi$ , and demand,  $\gamma$  factors are calculated by defining the probability of demand surpassing capacity in 50 years equal to 0.05%, 0.1%, 0.2%, 0.5%, and 1%. The results show that the  $\phi/\gamma$  decreases as  $R_{\mu}$  and  $\beta_{R,H\alpha}$  increases. The capacity and demand factors of spine-infill struts, spine-beams, and spine-columns for 0.1%  $P(D>C)_{50 \text{ years}}$  are:  $\gamma = 1.0$ ,  $\phi = 0.2$ ;  $\gamma = 1.0$ ,  $\phi = 1.0$ ;  $\gamma = 1.0$ ,  $\phi = 1.0$ ; respectively.

The thesis of Ni Made Novia Kusumayani is approved.

Scott J. Brandenburg

Thomas A. Sabol

John W. Wallace

Henry J. Burton, Committee Chair

University of California, Los Angeles  
2017

# Table of Contents

ABSTRACT OF THE THESIS .....	ii
List of Tables.....	vi
Acknowledgments .....	viii
1. INTRODUCTION .....	1
2. METHODOLOGY .....	6
2.1 Overview of Design Procedure for Rocking Spine System .....	6
2.2 The Reliability-Based Method (Victorsson, et al. 2013).....	10
2.3 Description of Building Case and Structural Modeling .....	16
3. ANALYSIS AND RESULTS .....	21
3.1 Response Spectrum Analysis .....	21
3.2 Incremental Dynamic Analysis .....	24
3.3 Reliability Analysis .....	27
4. CONCLUSIONS .....	38
REFERENCES.....	42

## List of Tables

Table 2. 1 Columns and Beams Dimension and Reinforcements, Burton et al. 2016 ...	18
Table 2. 2 Infill Strut Model Parameters, Burton et al. 2016 .....	20
Table 3. 1 The Yield Expected Story Shear, .....	23
Table 3. 2 The Yield Modification Factors, $R\mu$ , of the System .....	24
Table 3. 3 The Reliability Index, $\beta R, Ha$ .....	31
Table 3.4 Capacity and Demand Factors of Spine Infill Struts for 0.05% Probability of Demand Exceeding Capacity in 50 years .....	33
Table 3. 5 Capacity and Demand Factors of Spine Infill Struts for 0.1% Probability of Demand Exceeding Capacity in 50 years .....	34
Table 3. 6 Capacity and Demand Factors of Spine Infill Struts for 0.2% Probability of Demand Exceeding Capacity in 50 years .....	34
Table 3. 7 Capacity and Demand Factors of Spine Infill Struts for 0.5% Probability of Demand Exceeding Capacity in 50 years .....	34
Table 3. 8 Capacity and Demand Factors of Spine Infill Struts for 1% Probability of Demand Exceeding Capacity in 50 years .....	35
Table 3.9 Capacity and Demand Factors of Spine Beams for 0.1% Probability of Demand Exceeding Capacity in 50 years .....	36
Table 3.10 Capacity and Demand Factors of Spine Columns for 0.1% Probability of Demand Exceeding Capacity in 50 years .....	37



## List of Figures

Figure 1. 1 The Rocking Spine System (adapted from Burton et al. 2016) .....	3
Figure 2. 1 Loads Diagram on Rocking Spine After the Uplift (adapted from Burton et al. 2016) .....	7
Figure 2. 2 Characteristic Resistance for Log-normal Distribution .....	13
Figure 2. 3 The Comparison of The Design Story Shear, $V$ , to The Factored Nominal story shear strength, $\phi V$ , Victorsson et al. (2013) .....	14
Figure 2. 4 Typical Floor Plan of The Building (adapted from Burton et al. 2016) .....	17
Figure 2. 5 OpenSees Model (adapted from Burton et al. 2016) .....	19
Figure 3. 1 The Design Response Spectrum .....	21
Figure 3. 2 The Median of Maximum Spine Infill Struts Axial Forces .....	25
Figure 3. 3 The Median of Maximum Beams Hinge Moments.....	25
Figure 3. 4 The Median of Maximum Columns Hinge Moments.....	26
Figure 3. 5 The Log-Standard Deviation of Maximum Spine Infill Struts Axial Forces ..	26
Figure 3. 6 The Log-Standard Deviation of Maximum Beam Hinge Moments.....	27
Figure 3. 7 The Log-Standard Deviation of Maximum Column Hinge Moments.....	27
Figure 3. 8 Hazard Curves for Specified Site .....	30
Figure 3. 9 The Sensitivity of The Reliability Index, $\beta_R, Ha$ , to the $PCollD > CD > C$ ....	32
Figure 3. 10 The Sensitivity of $\phi/\gamma$ to $\rho$ Factor .....	36

## Acknowledgments

My study at University of California, Los Angeles (UCLA) was fully funded by the Indonesia Endowment Fund for Education (LPDP) under Indonesian Ministry of Finance, Education, and Religion. I am very blessed to be one of LPDP awardees and had an opportunity to enhance my knowledge and skill by studying abroad.

I would like to acknowledge some individuals who have contributed significantly to my thesis and education life in UCLA. First and foremost, I would like to thank my faculty and thesis advisor, Professor Henry J. Burton. I am very grateful to have an opportunity to work and learn from him. His discipline and enthusiasm to structural engineering inspire me to never stop learning and work harder to be a better engineer.

I would also like to thank Professor Scott J. Brandenburg, Thomas A. Sabol, and John W. Wallace for their commitment to serve as my thesis committee members. I am thankful for their time and valuable input. Thank you for the staff and faculty of the Department of Civil and Environmental Engineering at UCLA, especially to the Student Affairs Officers, Jesse Dieker and Lucy Capul, for being very helpful and informative in keeping my study target on track.

Finally, I would like to acknowledge my parents, Ni Nyoman Sukajani and Ketut Suma, my brother and sister in law, Wija and Ayu, and my dear friends for their endless pray and support. All of this would be impossible without them.

# 1. INTRODUCTION

Reinforced concrete frame buildings with infills are used worldwide because of their less expensive material cost and commonplace construction technique. As the demand for buildings is constantly increasing, these structures continue to grow, and nowadays infill frames are even implemented in taller buildings. This fact is raising a concern among experts since infill frames are generally constructed as low ductility system, which could lead to a significant risk of collapse under earthquake loading. The collapse cases for infill frames after the earthquakes in Haiti (2010), Italy (2009), China (2008), India (2001) and Turkey (1999) serve as evidence that if this type of structure would continue to be built, there should be a method to enhance its seismic performance.

Over the years, researchers have been developing seismic risk mitigation techniques to overcome the drawbacks of different types of masonry buildings. One approach that has been shown to improve the overall seismic performance is the introduction of a rocking infill wall into the system. Toranzo et al. (2001) conducted a study on rocking walls built from the confined-masonry that was integrated with hysteretic energy dissipators located at the base of the walls. The numerical analysis showed that the rocking wall design could satisfy the target drift and reduce damage in the structure under earthquake loading.

Mosalam and Günay (2009) conducted a study on retrofitting reinforced concrete frames with non-ductile infill walls by applying a rocking spine into the system. The retrofit methods included strengthening the non-ductile infill wall with mesh reinforcement and a concrete layer on one side of the wall. The additional reinforcement increases the vertical

forces from the infill panels to the column and can produce tensile forces in the column. By using a shallow foundation and letting the wall uplift, the strengthened wall would act as a rocking spine. The adequacy of the retrofit scheme was evaluated by non-linear dynamic analysis and the results showed that the retrofit scheme is effective for reducing the inter-story drift and produced a uniform drift along the height; therefore, the likelihood of a soft story failure can be reduced.

As an adaptation of the retrofit system proposed by Mosalam and Günay (2009), Burton et al. (2016) conducted a study to develop a design procedure for the rocking spine system in new infill frame buildings. As shown in Figure 1.1, the rocking spine system consists of a strong, stiff spine supported on a shallow foundation. In the Burton et al. (and current) study, the spine system was a reinforced concrete frame with strong masonry infills; however, a concrete shear wall could also be used as the spine. A rocking mechanism is activated when the overturning moment in the spine exceeds the overturning resistance, causing uplift at the shallow spine footing. The sources of overturning resistance include gravity loads acting directly on the spine and the kinematic restraint provided by the infill panels and beams adjacent to the spine. The spine overturning resistance also depends on the size of the footing at its base and the extent of vertical deformation in the soil.

In practice, the system may consist of multiple (orthogonal and parallel) adjacent bays that contribute to the overturning resistance of the system under earthquake loading. The spine-columns, spine-beams, and spine infills are expected to act as force-controlled

components, which remain essentially elastic under moderate earthquake. Meanwhile, adjacent beams and non-spine infills are designed as deformation-controlled elements which are expected to have inelastic deformation and dissipate energy under moderate earthquake. In the Burton et al. (2016) study, the rocking spine system was evaluated by non-linear static and dynamic analysis. The results show that the seismic design satisfies the drift limit in ASCE 7. The design has 2.8% probability of collapse at MCE hazard level for an ASCE Seismic Design Category D site, which is far less than the limit (10% probability of collapse at the MCE level) recommended in the FEMA P695 (FEMA, 2009) Guidelines.

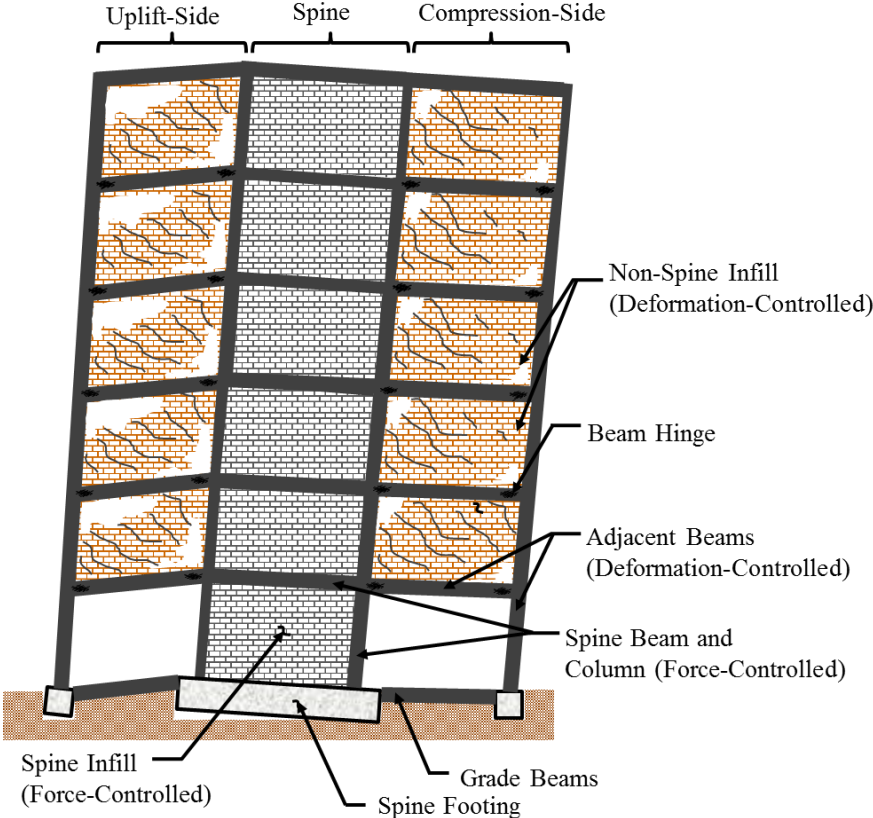


**Figure 1. 1** The Rocking Spine System (adapted from Burton et al. 2016)

Inspired by the capability of rocking spine system, this study is conducted with the purpose of establishing the demand and capacity factors for the force-controlled rocking spine elements using a reliability-based methodology. The approach used in this study, which is an adaptation of the Load and Resistance Factor Design (LRFD) methodology, was developed by Victorsson, et al (2013) and applied to special concentric braced frame connections. The capacity-based design requirements are resolved by considering the variability of demands and component capacity along with target reliability. The differences between the reliability and LRFD method are in the way of defining demands and reliability index,  $\beta$ . In LRFD method, demands are taken directly from the median of the load effect, such as dead load, live load, and other loads. Meanwhile, in reliability method, demands are determined by considering four variabilities, which are the ratio of statistical demand value from nonlinear dynamic analysis at MCE level, the material strength, geometrical properties, and record-to-record variability. Reliability index,  $\beta$  in the reliability method are chosen from the average values in structural design prior to LRFD. In the reliability method,  $\beta$  are calculated by considering the yield modification factor of the system,  $R$ , and the hazard curve of the site location,  $H_a$  (Victorsson, 2013).

The first main step of this study is constructing a two-dimensional model of the reinforced concrete frame with rocking spine system in OpenSees and performing Incremental Dynamic Analysis (IDAs) (Vamvatsikos and Cornell, 2002) using a suite of ground motions. The maximum induced force demands in the force-controlled spine components are recorded and the median values are determined. The next step is to determine the target reliability index of the system,  $\beta_{R,H_a}$ . The subscripts in the reliability index refers to

the site's ground motion hazard and the R-factor used to design the structure. Once the medians of the maximum induced forces are available and the reliability index is chosen, the demand and capacity factors could be calculated by adjusting the tolerable probability of collapse due to the failure of capacity-designed components to the target probability of collapse on the relevant building code.

## 2. METHODOLOGY

### 2.1 Overview of Design Procedure for Rocking Spine System

The main steps in the design methodology proposed by Burton et al. (2016) consist of defining the required overturning resistance of rocking spine system and detailing the key elements to prevent undesirable failure mechanisms. The overturning moment before uplift is provided by the gravity load on the spine, and after uplift, the beams and infills at adjacent bays provide the resistance by acting like an outrigger system. The idealized free-body diagram of the rocking spine is presented in Figure 2.1.

The minimum overturning moment resistance of rocking spine system is determined by using the equivalent lateral force procedure as outlined in ASCE 7-10. Using the design spectra and the response modification factor,  $R$ , the required design based shear and the equivalent lateral forces are calculated. The summation of the multiplication of equivalent lateral forces,  $F_i$ , to the height of those lateral forces,  $H_i$ , for all floors will give the required overturning moment resistance,  $M_u$ , which should be less than the nominal overturning resistance reduced by the strength reduction factor,  $\phi M_n$ . The nominal overturning moment resistance is determined by taking the contribution of the adjacent beams,  $M_{bU}$  and  $M_{bC}$  and non-spine infill struts,  $P_{sU}$  and  $P_{sC}$ , into consideration.



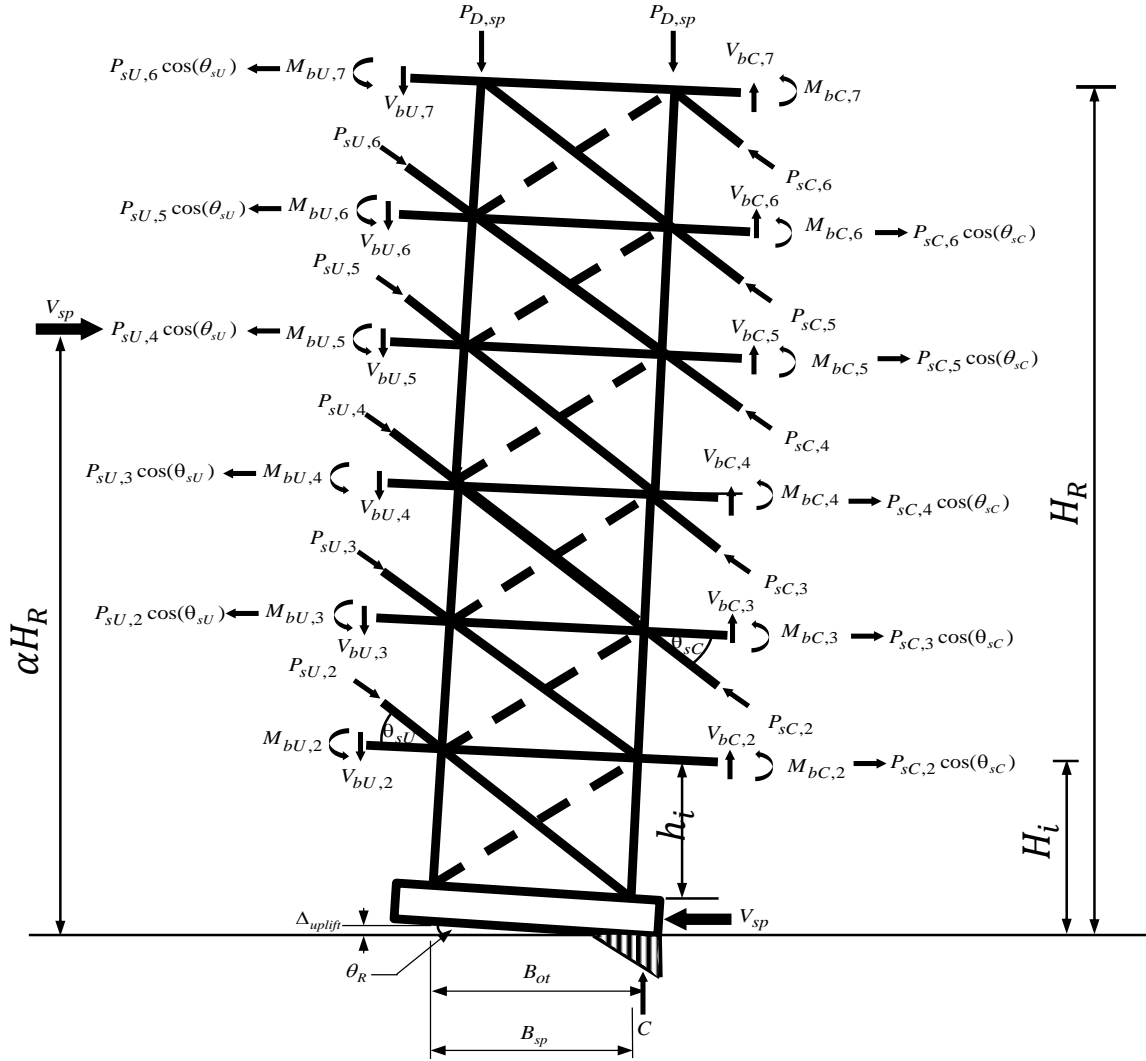


**Figure 2. 1** Loads Diagram on Rocking Spine After the Uplift (adapted from Burton et al. 2016)

Burton et al. (2016) proposed equations to determine the overturning moment resistance of rocking spine systems,  $M_{res}$ .

$$M_{res} = M_{res,D} + M_{res,bU} + M_{res,bC} + M_{res,sU} + M_{res,sC} \quad (1)$$

$M_{res,D}$  is the overturning resistance by considering the expected gravity loads on the columns at the uplift side,  $P_{D,sp}$  and the horizontal length from the tension column to

the center of rotation,  $B_{ot}$ . In this study, the  $B_{ot}$  is taken equal to the span of the spine system.

$$M_{res,D} = P_{D,sp} B_{ot} \quad (2)$$

$M_{res,bU}$  and  $M_{res,bC}$  are the overturning resistance coming from the adjacent beams that are framing into the columns at the uplift side and compression side, respectively. Since this study is analyzing the 2-D frame of the system,  $M_{res,bU}$  do not consider the contribution of the beams that are orthogonal with the spine columns.  $M_{res,bU}$  and  $M_{res,bC}$  in the rocking spine system are calculated by equations (3) and (4), respectively.  $nbU$  and  $nbC$  are the number of beams framing into the columns at the uplift side and compression side, respectively,  $M_{bU}$  and  $M_{bC}$  are the expected yield end moments of the adjacent beams at the uplift side and compression sides, respectively, and  $L_{bU}$  is the length of the adjacent beams.

$$M_{res,bU} = \sum_{i=1}^{nbU} \left( M_{bU,i} + \frac{2M_{bU,i}}{L_{bU,i}} B_{ot} \right) \quad (3)$$

$$M_{res,bC} = \sum_{i=1}^{nbC} (M_{bC,i}) \quad (4)$$

$M_{res,sU}$  and  $M_{res,sC}$  are the overturning resistance from the expected axial strength of the non-spine infill panel at the uplift side,  $P_{sU}$ , and compression side,  $P_{sC}$ , respectively. The same as the  $M_{res,bU}$ ,  $M_{res,sU}$  in this study is considering only the contribution of the non-spine infills panels that are parallel with the uplift columns. Equations (5) and (6) describe the relationship of axial forces to the  $M_{res,sU}$  and

$M_{res,SC}$ , respectively.  $nsU$  and  $nsC$  are the number of struts in the uplift and compression sides, respectively,  $\theta_{sU}$  and  $\theta_{sC}$  is the angle of the struts in uplift and compression sides to the horizontal direction, respectively, and  $h$  is the inter-story height.

$$M_{res,sU} = \sum_{i=1}^{nsU} (P_{sU,i} \sin(\theta_{sU,i}) B_{ot}) + \sum_{i=1}^{nsU} (P_{sU,i} \cos(\theta_{sU,i}) h_i) \quad (5)$$

$$M_{res,sC} = \sum_{i=1}^{nsC} (P_{sC,i} \cos(\theta_{sC,i}) h_i) \quad (6)$$

In order to consider the P-delta effect of the system, the net overturning resistance,  $M_{res}^*$ , is calculated by equation (7) where  $w_i$  is the seismic weight at each floor,  $H_i$  is the height from the base to the specified floor, and  $\theta_R$  is the rocking angle:

$$M_{res}^* = M_{res} - \theta_R \sum_{i=1}^{nfloor} w_i H_i \quad (7)$$

By assuming the distribution of shear strength is triangular for the first dominant mode, the equivalent lateral base shear of spine,  $V_{sp}$ , can be calculated by equation (8), where  $\alpha H$  is the distance from the base to the lateral force which is taken equal to two third of system's total height.

$$V_{sp} = \frac{M_{res}^*}{\alpha H} \quad (8)$$

After the spine required overturning strength has been determined, the drift demand under the MCE level intensity is evaluated and compared with the relevant building code limits. Once the drift limit is satisfied through an iterative process, the design and detailing of the structural components can be performed. In general, the design of the key elements in rocking spine system is conducted by assuming the spine system components; spine infill panels, spine beams and columns, act as force-controlled components and the adjacent beams and the non-spine infill panels as deformation-controlled components. The force-controlled components are expected to remain essentially elastic and have minimal damage under a moderate earthquake. Meanwhile the deformation-controlled components are expected to experience inelastic deformation and dissipate energy under the earthquake loading. For the spine, the element forces and moments are determined from gravity load, the equivalent lateral force distribution and the system's overturning strength, i.e. a capacity-design approach (Burton, 2014).

## 2.2 The Reliability-Based Method (Victorsson, et al. 2013)

The goal of the reliability-based method proposed by Victorsson et al. (2013) is to establish the load and resistance factors for force-controlled components in seismic lateral force resisting systems. The basic equation used to determine the capacity( $\phi$ ) and demand ( $\gamma$ ) factors is:

$$\frac{\gamma}{\phi} = \frac{\hat{D}_m C_n}{D_n \hat{C}_m} \exp\left(\beta_{R,Ha} \sqrt{V_C^2 + V_D^2 - 2\rho V_C V_D}\right) \quad (9)$$

This equation is formulated based on the assumption that the demand and capacity probability are lognormally distributed.  $\hat{D}_m$  and  $\hat{C}_m$  are median values of the demand and capacity probability distribution respectively, while  $D_n$  and  $C_n$  are nominal values of the demand and capacity probability distribution, respectively. The median demands for the analysis are taken from induced forces in force-controlled components at the MCE level intensity. In the rocking spine system study, MCE level intensity is taken equal to 1.3 g.  $\beta_{R,Ha}$  is the reliability index that is related to the probability of the demand exceeding the capacity in force-controlled components. The subscripts of the reliability index represent the effect of the R-factor and the site ground motion's hazard curve (Ha).  $V_C$  and  $V_D$  represent the log-normal standard deviation of the capacity and demand distributions respectively, and  $\rho$  is the correlation between demand and capacity.

In this study,  $\frac{\hat{D}_m}{D_n}$  are estimated from the multiplication of load model parameter variable, material strength variable, fabrication variable, and record to record variable. The load model parameters are defined as the ratio of induced force in force-controlled element at MCE level ground motion from non-linear response history analysis to strengths predicted by nominal equations (Victorsson, 2013). The induced forces are controlled by the force demands that could cause yielding in the deformation-controlled components. Incremental Dynamic Analysis (IDAs) (Vamvatsikos and Cornell, 2002) are performed to generate the force demands needed for the reliability assessment. In this study the variable of material strength,

fabrication, and record to record are taken equal to 1.0; in other words, they do not affect the  $\frac{\hat{D}_m}{D_n}$  values.

The  $\frac{\hat{C}_m}{C_n}$  are calculated from the multiplication of the component model variable, the material strength variable, and the fabrication variable (Victorsson, 2013). In this study, the variable of material strength and fabrication are taken equal to 1.0, meanwhile the component model variables are determined by the ratio of the median of capacity strength from the test data to the expected strength from nominal strength equations. The expected strengths of the material are determined by using the concept of characteristic values. The characteristic values are calibrated by specifying the probability of non-exceedance. For the characteristic resistance, the values are expected to be slightly less than the mean values. A 5 % probability of non-exceedance is assumed to determine these values. Figure 2.2 describes the characteristic resistance with the assumption that the values are log-normally distributed. The characteristic resistances,  $r_k$ , are calculated by the following equations:

$$P(R < r_k) = \Phi\left(\frac{\ln r_k - \mu_{\ln R}}{\sigma_{\ln R}}\right) \quad (10)$$

where  $\mu_{\ln R}$  is the log-mean of the capacity and  $\sigma_{\ln R}$  is the log-standard deviation of the capacity. The  $P(R < r_k)$  is equal to 0.05.

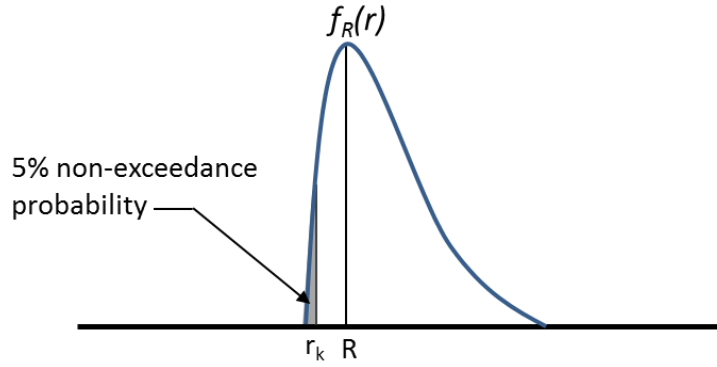


**Figure 2. 2** Characteristic Resistance for Log-normal Distribution

The reliability index,  $\beta_{R,H\alpha}$ , is determined by considering the system R-factor and member over-strength, the site's ground motion hazard curve, the effect of force-controlled components failures to the system's collapse, and the tolerable probability of collapse caused by the demand exceeding the capacity in the force-controlled components.  $\beta_{R,H\alpha}$  is calculated as the inverse of standard normal cumulative distribution function in the following equation:

$$\beta_{R,H\alpha} = \Phi^{-1} \left( \frac{MAF(D > C)}{MAF(Sa > Sa_{y,exp})} \right) \quad (11)$$

The  $MAF(Sa > Sa_{y,exp})$  is the mean annual frequency of the ground motion intensity exceeding the ground motion intensity that initiates yielding in the deformation-controlled components. This value is obtained from the site's ground motion hazard curve.  $Sa_{y,exp}$  is determined by considering the R-factor and members over-strength that are represented by the yield modification factor,  $R_\mu$ . The yield modification factor,  $R_\mu$  can be defined by the ratio of the elastic story shear design demand,  $V_{DBE}$

and the expected yield story shear,  $V_{y,exp}$ . The  $R_\mu$  factor is a convenient way to estimate  $Sa_{y,exp}$  in order to investigate the likelihood of designed story shear strength is exceeded.

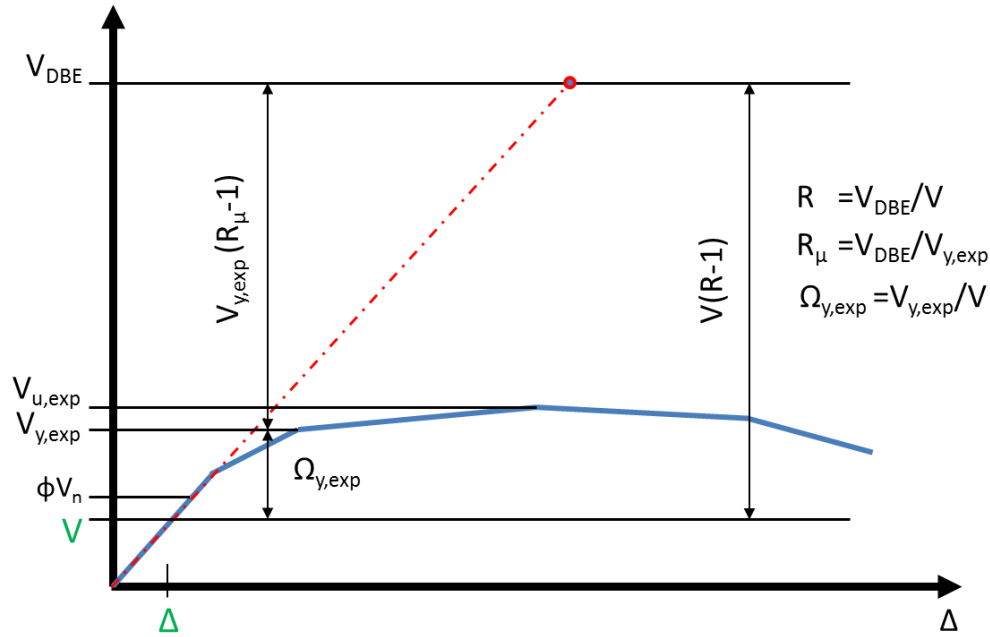


**Figure 2. 3** The Comparison of The Design Story Shear,  $V$ , to The Factored Nominal story shear strength,  $\phi V$ , Victorsson et al. (2013)

Victorsson et al. (2013) proposed the procedure to determine the yield modification factor,  $R_\mu$ , of the system. The procedure includes conducting a response spectrum analysis using the DBE response spectrum to generate the story shear force,  $V_{DBE}$ . The DBE response spectrum is generated by taking the  $S_{DS}$  value equal to two-third of the  $S_{MS}$  value. The design story shear,  $V$ , obtained by dividing the  $V_{DBE}$  by the response modification factor,  $R$ . Equations (12) and (13) provide the relation of the  $Sa_{y,exp}$  and  $R_\mu$ .



$$Sa_{y,exp} = \frac{Sa_{DBE}}{R} * \left( \frac{V_{y,exp}}{V} \right) \quad (12)$$

$$R_{\mu} = \frac{Sa_{DBE}}{Sa_{y,exp}} \quad (13)$$

$Sa_{DBE}$  refers to the DBE spectral intensity and  $V_{y,exp}$  refers to the expected yield strength of the system.  $V_{y,exp}$  is calculated from the equivalent lateral base shear resistance,  $V_{sp}$  which is determined from overturning moment resistance of the rocking spine provided by the gravity loads on the uplift sides, the end moments of adjacent beams framing into the spine columns at the uplift and compression sides, and the axial forces in the non-spine infill struts at the uplift and compression sides. The P-Delta effect is considered in this study.  $V_{sp}$  is determined by following the procedure in the section 2.1; equations (1) to (8).

The  $MAF(D>C)$  is the mean annual frequency of demand exceeding capacity. This value is calculated by considering the tolerable probability of collapse caused by the force-controlled component failure in 50 years and the influence of the demand exceeding capacity in the capacity-designed components to the system collapse safety. The equation to calculate the annual frequency of demand surpassing the capacity is derived from the Poisson process as presented below.

$$P(Collapse)_{50\ years} = 1 - e^{-50MAF(Collapse)} \quad (14)$$

$$\Delta P(Coll_{D>C})_{50\ years} = 1 - e^{-50P(Coll_{D>C}|D>C) \times MAF(D>C)} \quad (15)$$

$$MAF(D > C) = \frac{-\ln((1 - \Delta P(Coll_{D>C})_{50\ years}))}{50P(Coll_{D>C}|D > C)} \quad (16)$$

$P(\text{Collapse})_{50 \text{ years}}$  is the 50-year probability of collapse,  $MAF(\text{Collapse})$  is the mean annual frequency of collapse,  $P(\text{Coll}_{D>C}|D > C)$  is the probability of collapse conditioned on the failure of a force-controlled components and  $\Delta P(\text{Coll}_{D>C})_{50 \text{ years}}$  is the additional contribution of collapse due to failure of a force-controlled component in 50 years. The tolerable additional contribution to the probability of collapse in 50 years caused by force-controlled-component-failure depends on the code developer's expectation. The FEMA P695 guidelines and new target risk design maps could be used to define the recommended value. Victorsson et al. (2013) provides a more detailed derivation of the reliability index in the Chapter 3 of his thesis dissertation from the equation (3-5) to (3-21).

## **2.3 Description of Building Case and Structural Modeling**

The floor plan of the building case considered in this study is presented in Figure 2.5. It is a six-story building with 12 ft typical floor to floor height. The building consists of 4 rocking spine bays in each direction. The building is assumed to be located in a high seismic region with  $S_{MS}=1.5 \text{ g}$  and  $S_{M1}=0.9 \text{ g}$ . The fundamental period of the building calculated using ASCE 7 is equal to 0.7 sec. The response modification factor,  $R= 6$ , is assumed for the building (Burton et al., 2016).

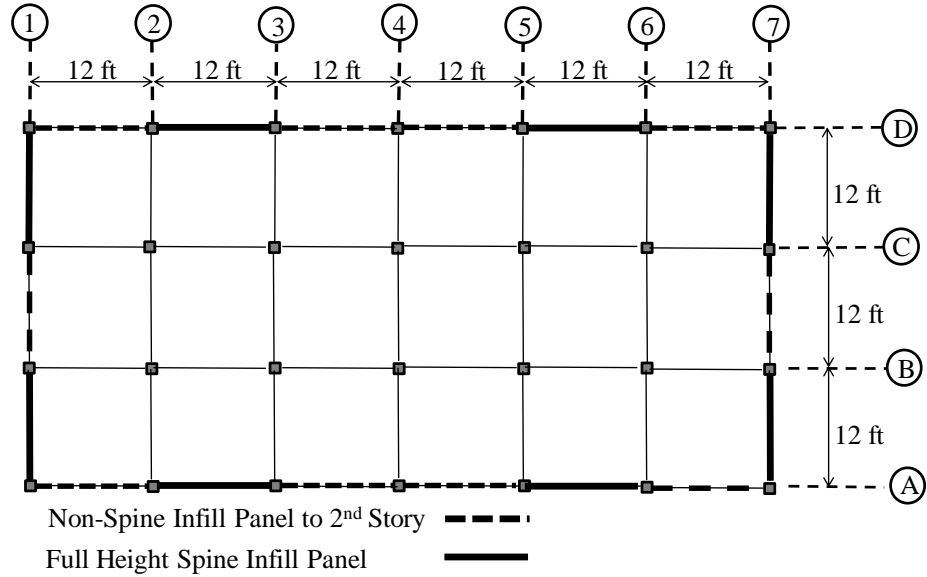


**Figure 2. 4** Typical Floor Plan of The Building (adapted from Burton et al. 2016)

The struts, beam and column sizes are determined from the design procedure described previously in section 2.1. The non-spine infill panels have a prism compressive strength of  $f'_m = 0.508 \text{ ksi}$ . The reinforced concrete components are designed with a concrete compressive strength equal to 3 ksi and steel rebar with 60 ksi minimum yield strength. The details about columns and beam designs are summarized in the Table 2.1.

**Table 2. 1** Columns and Beams Dimension and Reinforcements, Burton et al. 2016

Section	Dimension	Long. Reinforcement	Stirrup
Spine Columns	30 in x 30 in	12#8	#4@12 in
Non-Spine Columns, from the ground to the 3 <sup>rd</sup> floor	18 in x 18 in	8#6	#4@12 in
Non-Spine Columns, from the 4 <sup>th</sup> floor to the 6 <sup>th</sup> floor	14 in x 14 in	8#5	#4@12 in
Beam	14 in x 18 in	5#6, top and bottom	#4@4 in, in the hinge region #4@8 in, outside the hinge region

A two-dimensional model of frame line A is constructed in OpenSees, which consists of a six-bay, 6-story reinforced concrete frame with two-rocking spine bays supported on shallow foundations. The spines are located at the 2<sup>nd</sup> and 5<sup>th</sup> bays. Leaning columns are used to capture P- $\Delta$  effects from gravity loads included in the model.

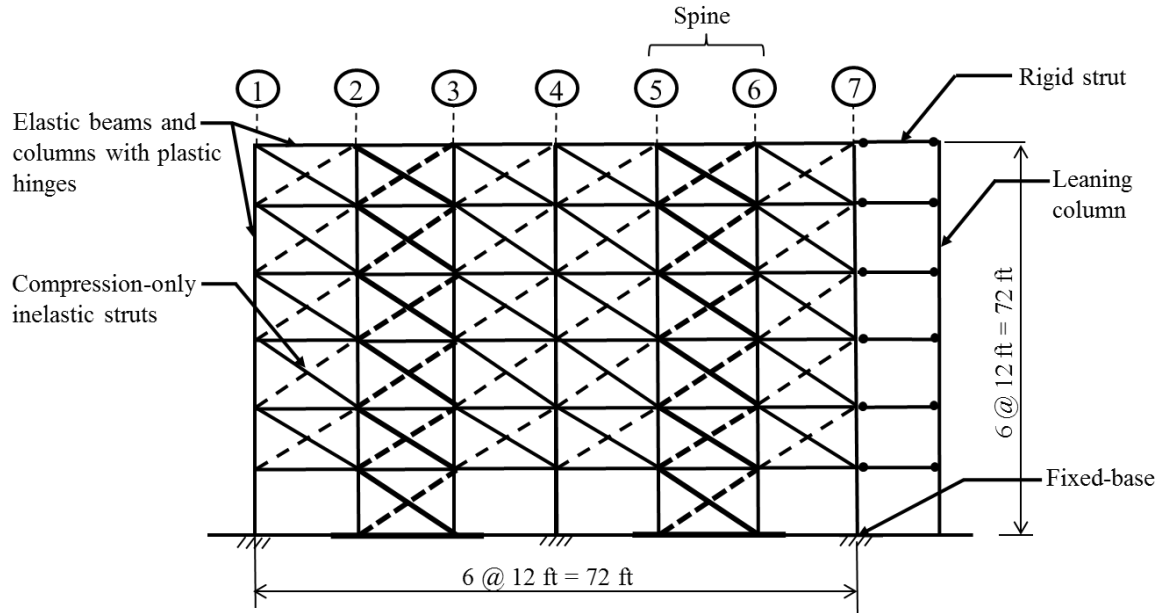


**Figure 2. 5** OpenSees Model (adapted from Burton et al. 2016)

The adjacent (deformation-controlled) beams and columns are modeled as elastic elements with the flexural hinges with the Ibarra-Krawinkler hysteretic model (Ibarra et al. 2005). The flexural hinge model parameters are based on the empirical relationships developed by Haselton et al. (2008). The non-spine (deformation-controlled) infill panels are modeled using nonlinear axial struts with the strength and stiffness computed using the analytical method by Saneinejad and Hobbs (1995). The other parameters, such as such as the ratio of post-capping force to yield force,  $F_c/F_y$ , the ratio of capping deformation to yield deformation,  $\Delta_c/\Delta_y$ , and the ratio of post-capping stiffness to yield stiffness,  $K_p/K_e$ , are calculated from the guidelines by Burton and Deierlein (2016). Table 2.2 summarizes the infill strut parameters. The spine infill (force-controlled) is modeled using elastic struts and the nonlinear flexural hinges are not incorporated in the spine beam elements (force-controlled).

**Table 2. 2** Infill Strut Model Parameters, Burton et al. 2016

Infill Type	$K_e$ (kip/in)	$F_y$ (kips)	$F_c/F_y$	$\Delta_c/\Delta_y$	$K_c/K_y$
Non-spine	251	30	1.4	4.5	-0.15
Spine	965	162	1.4	4.5	-0.15

### 3. ANALYSIS AND RESULTS

#### 3.1 Response Spectrum Analysis

Response Spectrum Analysis (RSA) is performed on a 1-bay rocking spine with one adjacent non-spine frame on each side. The purpose of the RSA is to obtain the yield modification factors of the building,  $R_{\mu}$ , and the ground motion intensity that caused yielding in the deformation-controlled component,  $Sa_{y,exp}$ . The design basis earthquake (DBE) response spectrum is developed based on ASCE 7 with the data available from the rocking spine system model shown in the study conducted by Burton et al. (2016). The  $S_{DS}$  is two third of the  $S_{MS}$  and the fundamental period of the system is  $T_1=0.7$  sec.

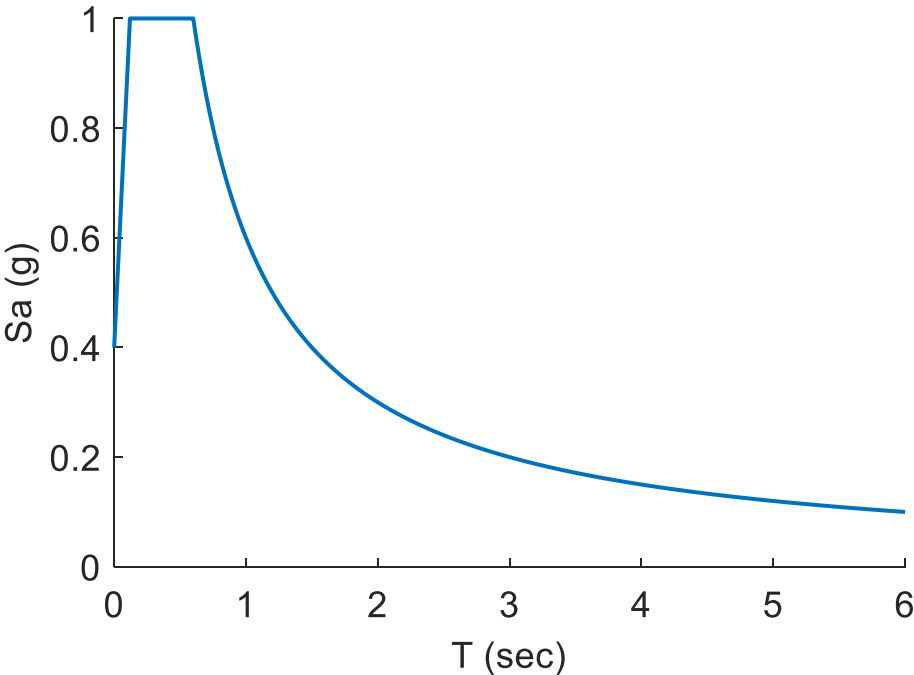


**Figure 3. 1** The Design Response Spectrum

By using ETABS, the RSA is performed and the story shear for each floor is recorded. The story shear from ETABS,  $V_{DBE}$ , is divided by the response modification factor,  $R$ , of the system and called  $V$ .

$Sa_{y,exp}$  is estimated by multiplying the ratio of DBE spectral intensity and modification factor,  $Sa_{DBE}/R$ , by the ratio of  $V_{y,exp}$  and  $V$ ; equation (12).  $V_{y,exp}$  is the expected yield shear force for each story computed by considering the overturning moment resistance of rocking spine system described in equations (1) to (8) in this report. The expected dead load on the spine columns,  $P_{D,sp}$  are determined from the total seismic weight of the building, 3062 kips, and the tributary area.  $M_{bU}$  and  $M_{bC}$  are determined from the expected yield moment of the proposed adjacent beams which equal to 1809 kip-ft.  $P_{sU}$  and  $P_{sC}$  are determined from the expected yield strength of non-spine infill struts,  $F_y$  (Table 2.2). With  $B_{ot}$  equal to 12 ft, the total overturning moment resistance,  $M_{res}$  of the system is calculated equal to 8457 k-ft. The rocking angle,  $\theta_R$ , of the system is 0.4% determined from the drift ratio at the onset of strength degradation in the non-spine infill at the uplift side (Burton et al, 2016). The net overturning moment resistance,  $M_{res}^*$  is calculated by putting the P-Delta effect into the consideration, which is equal to 8200 k-ft and the expected lateral base shear of the rocking spine system,  $V_{sp}$  is equal to 171 kips. With the assumption that the expected lateral base shear is distributed by following the equivalent lateral force procedure in ASCE 7-10, the  $V_{y,exp}$  for each story are presented in Table 3.1.  $k$  factor for  $T_1 = 0.7$  sec is 1.1 and Since there are two lateral resisting system in x-direction, the system only using half of the total seismic weight.



**Table 3. 1** The Yield Expected Story Shear,

Story	$w_i$ (kips)	$H_i$ (ft)	$H_i^k$	$w_i H_i^k$	$F = \frac{w_i h_i^k}{\sum w_i h_i^k} V_{Sp}$ (kips)	$V_{y,exp}$ (kips)
6	255	72	79	20208	49	49
5	255	60	66	16840	41	89
4	255	48	53	13472	33	122
3	255	36	40	10104	24	146
2	255	24	26	6736	16	163
1	255	12	13	3368	8	171
$\sum_{i=1}^{nfloor} w_i$	<b>1531</b>	$\sum_{i=1}^{nfloor} w_i H_i^k$		<b>70729</b>		

From results in Table 3.1,  $Sa_{y,exp}$  and  $R_\mu$  are calculated by following equations (12) and (13), respectively. Using  $Sa_{DBE}$  equal to 0.9 g, the yield response modification factor for each floor are presented in Table 3.2. The results show that  $Sa_{y,exp}$  are the same for each floor, meaning yielding in the deformation-controlled components happen at the same time. Victorsson et al (2013) described an optimal design as a system that has a  $R/R_\mu$  in the range of 1.5 – 2.0. The system has  $R/R_\mu=1.6$ ; therefore, the proposed design of rocking spine system is considered optimum.

**Table 3. 2** The Yield Modification Factors,  $R_\mu$ , of the System

Story	Story Shear, $V_{RSA}$ (kips)	$V_{y,exp}$	$V_{y,exp}/V_{RSA}$	$Sa_{y,exp}$	$R_\mu$
6	30	49	1.6	0.2	3.7
5	55	89	1.6	0.2	3.7
4	75	122	1.6	0.2	3.7
3	91	146	1.6	0.2	3.8
2	102	163	1.6	0.2	3.8
1	108	171	1.6	0.2	3.8

### 3.2 Incremental Dynamic Analysis

Incremental dynamic analysis (IDA) is performed in OpenSees with the 44 FEMA P695 ground motions. The purpose of this analysis is to determine the demands in the force-controlled components. The median of maximum axial forces of the infill struts, beam hinge moments, and column hinge moments, normalized by their expected yield strength are plotted versus spectral acceleration in Figure 3.2, 3.3 and 3.4 respectively. Meanwhile, the log-standard deviations of the corresponding induced force are presented in Figure 3.5 – 3.7.

The trends show that the first story has the largest demand for each force-controlled component. The normalized values of infill struts are much higher than the normalized values of beams and columns. The dispersions for the three components at the MCE level varies from 0.11-0.38. The median values and log-standard deviation of the demands at the MCE level, 1.3 g, are calculated and referred as  $\hat{D}_m$  values and  $V_D$ , respectively.

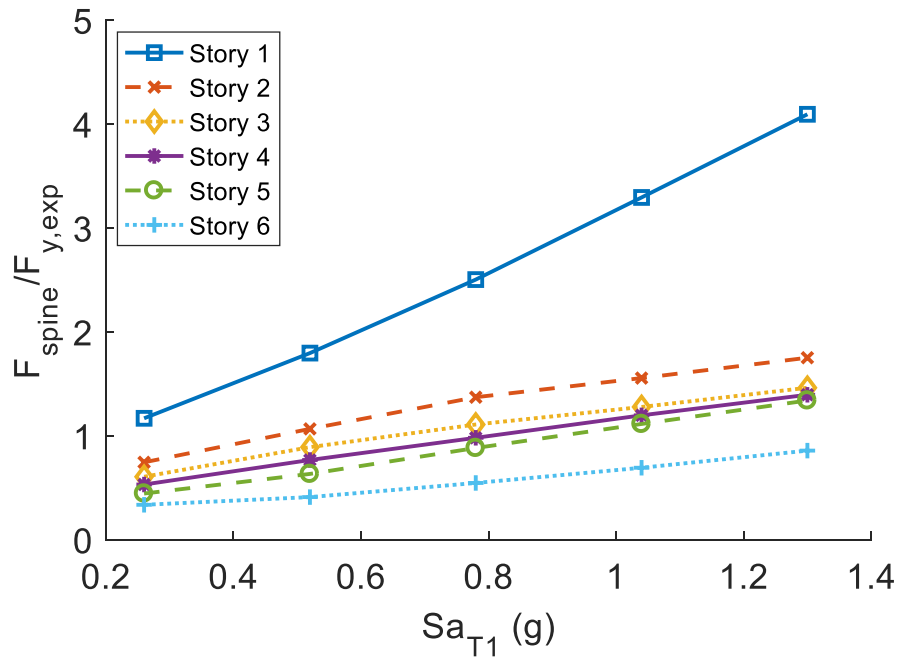


**Figure 3. 2** The Median of Maximum Spine Infill Struts Axial Forces

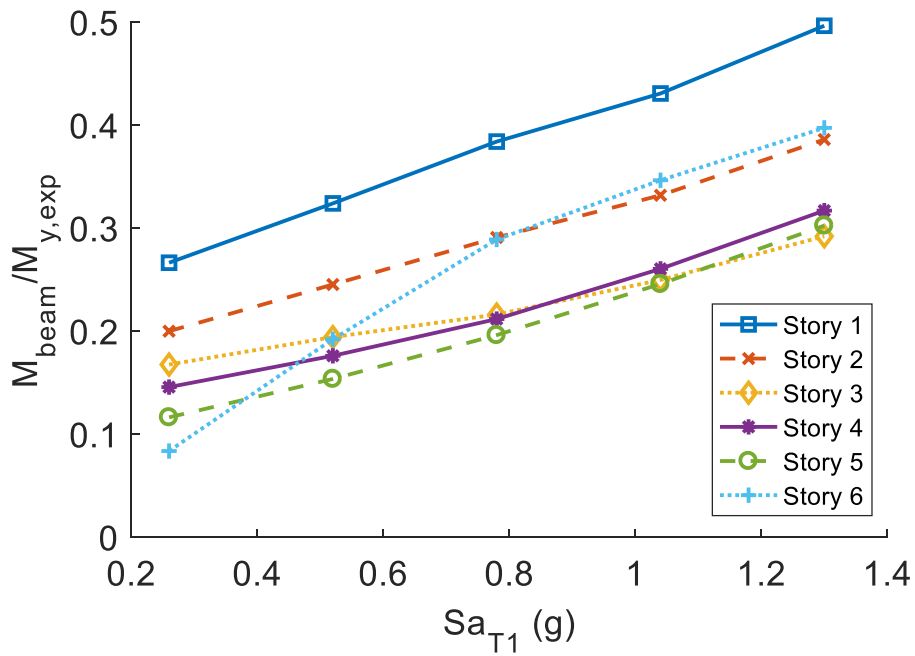


**Figure 3. 3** The Median of Maximum Beams Hinge Moments

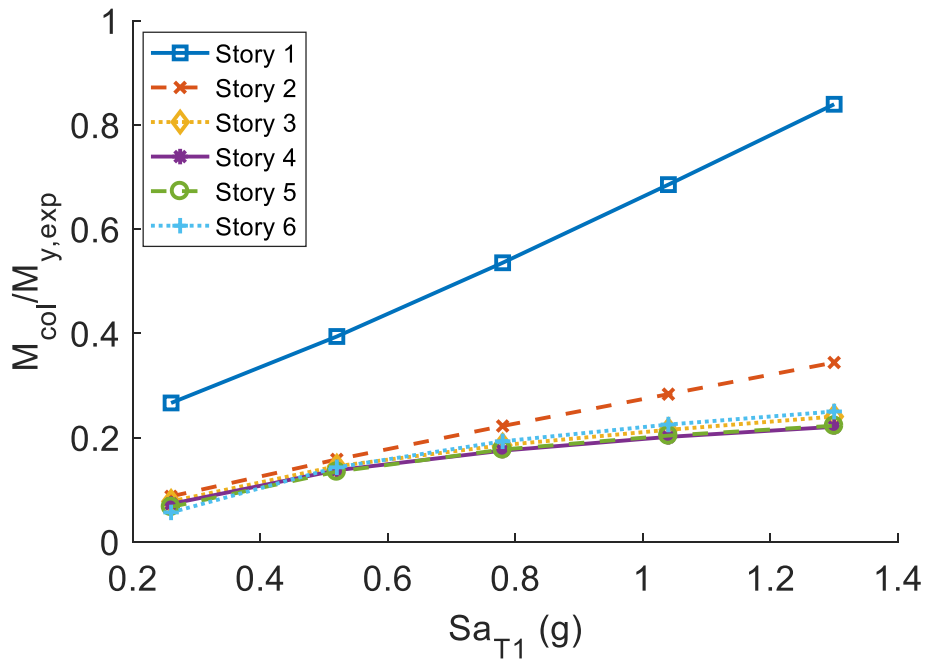


**Figure 3. 4** The Median of Maximum Columns Hinge Moments

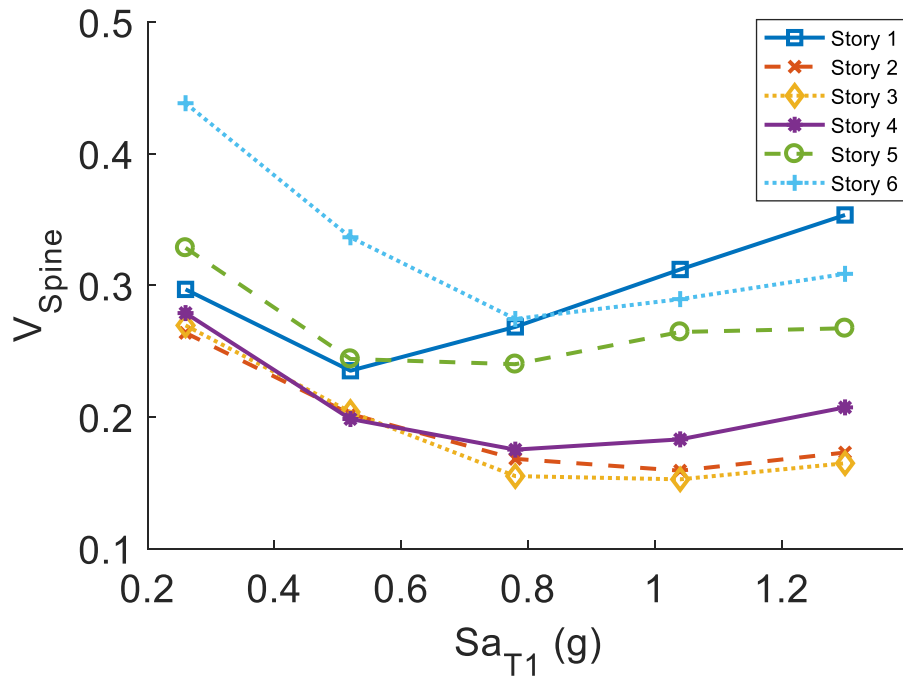


**Figure 3. 5** The Log-Standard Deviation of Maximum Spine Infill Struts Axial Forces

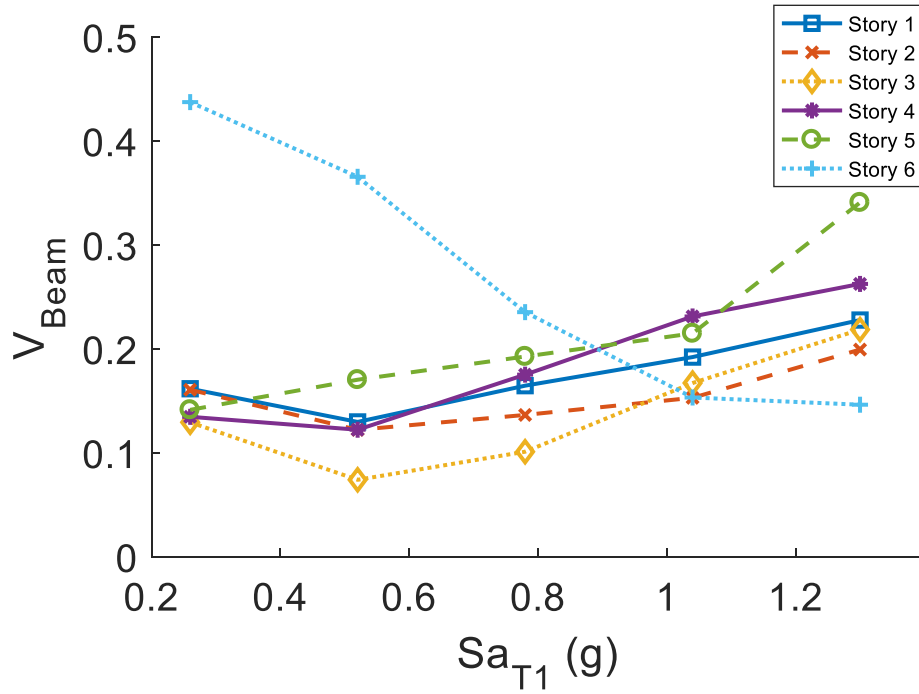


Figure 3. 6 The Log-Standard Deviation of Maximum Beam Hinge Moments

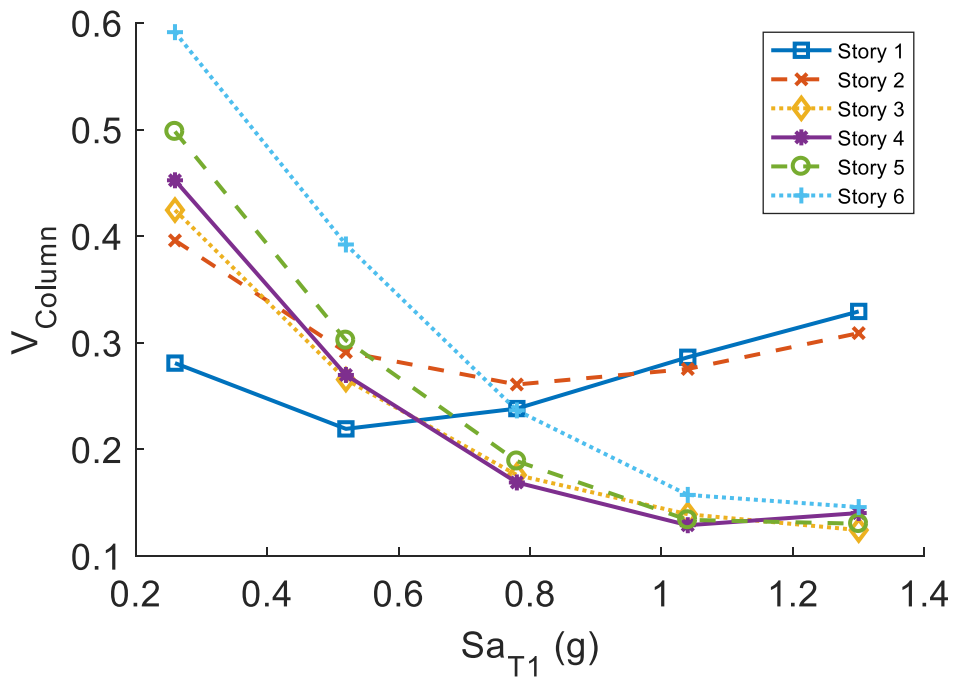


Figure 3. 7 The Log-Standard Deviation of Maximum Column Hinge Moments

### 3.3 Reliability Analysis

This analysis is conducted to determine the demand and capacity factors of the force-controlled components of concrete frames with rocking spine systems. The demand and capacity factors are calculated using equation (9). As mentioned previously in Section 2.2, the ratio of median demands and nominal demands,  $\hat{D}_m/D_n$  are determined by the ratio of induced forces in the force-controlled components at the MCE level intensity from incremental dynamic analysis to their predicted strength. The ratio of the median and nominal capacity,  $\hat{C}_m/C_n$ , is equal to 1.5, which obtained from the ratio of the expected strength of force-controlled components and the characteristic capacity,  $r_k$  that has a 5% non-exceedance probability.

The log-standard deviations of the demands,  $V_D$ , are determined from the dispersion of the IDA results at the MCE level ground motion, and since there is not sufficient test data provided for the capacity, the log-standard deviation of the capacity,  $V_C$ , is taken by following the suggested values by Victorsson et. al (2013) for non-ductile failure mode which is equal to 0.25.

The reliability index,  $\beta_{R,Ha}$ , is defined by considering the mean annual frequency of demands in the components exceeding capacity,  $MAF(D > C)$ , and the mean annual frequency of the ground motion intensities exceeding the intensity that caused yield at deformation-controlled components,  $MAF(Sa > Sa_{y,exp})$ . The  $MAF(D > C)$  is based on the tolerable added probability of collapse due to the failure of force-controlled components in 50 years. Determining the tolerable added

probability of collapse due to the failure of the force-controlled component is somewhat subjective. For example, the new risk-targeted design maps in ASCE 7-10 are based on a collapse risk threshold for a modern code-conforming structure of 1% probability of collapse in 50 years. This upper limit is based on collapse analyses that did not consider the failure of force-controlled components. One must therefore decide, how much additional collapse risk due to the failure of the force-controlled components  $\Delta P(Coll_{D>C})_{50\ years}$  that is tolerable. In this study, we consider a range of  $\Delta P(Coll_{D>C})_{50\ years}$  values: 0.05%, 0.1%, 0.2%, 0.5%, and 1%, which correspond to total collapse risk thresholds ( $P(Collapse)_{50\ years}$ ) of 1.05%, 1.1%, 1.2%, 1.5%, and 2% respectively.

As shown in equation (16),  $MAF(D > C)$  also depends on the likelihood that the structures collapse given the failure of the force-controlled components,  $P(Coll_{D>C}|D > C)$ . This can be explicitly computed by conducting a collapse performance assessment considering the nonlinearity in the spine components. However, in this study, an initial (conservative) assumption will be made on the value of  $P(Coll_{D>C}|D > C)$  and we will explore the sensitivity of  $MAF(D > C)$  to this assumed value.

The mean annual frequency of the ground motion's intensities,  $S_a$ , surpassing the intensity that causes yielding in the deformation-controlled components,  $S_{a,y,exp}$ , is obtained from the site's ground motion hazard curve. The adopted hazard curve was obtained from the OpenSHA software for a site located at coordinate

34.615°N, 117.802°W with  $S_a$  period= 0.75 second (close to the code period of the considered building). This site's seismic parameters ( $S_{MS}$  and  $S_{M1}$ ) are the same as what was used to design the building.

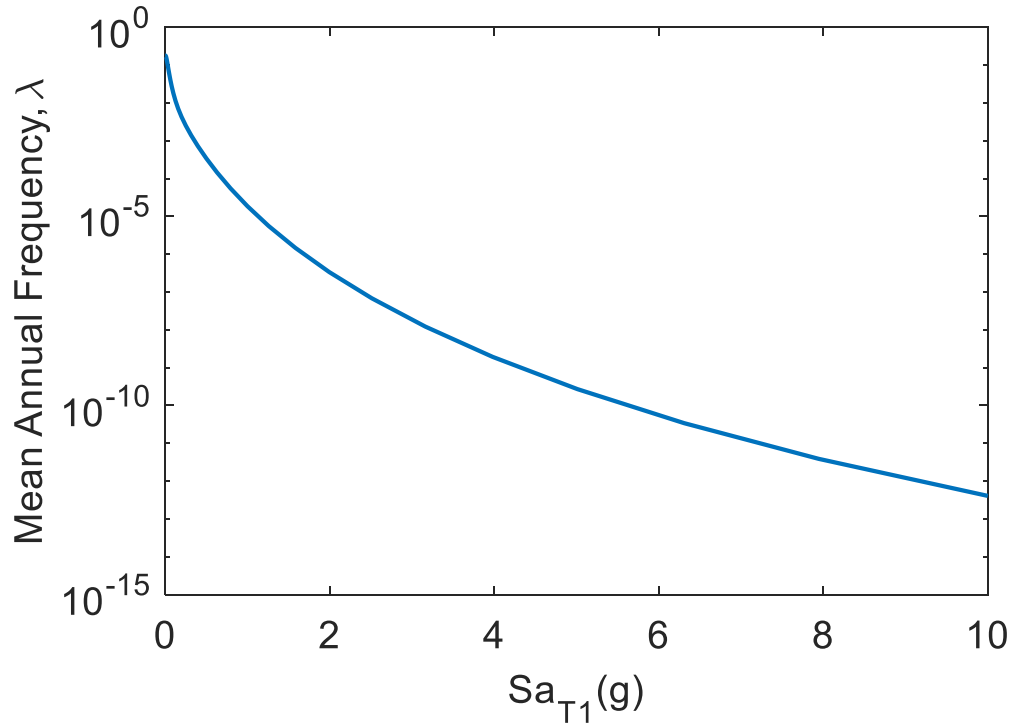


**Figure 3. 8** Hazard Curves for Specified Site

Using the  $MAF(S_a > S_{a_{y,exp}})$  collected from the ground motions hazard curve and assuming  $P(Coll_{D>C} | D > C) = 1$ , the reliability index,  $\beta_{R,Ha}$ , are calculated using equations (11) and (16) for each story and summarized in Table 3.2.

As described in Section 3.1,  $R_\mu$  is useful for keeping track of  $S_{a_{y,exp}}$  which is essential for evaluating the likelihood of the system experiencing the design forces. Since the  $R_\mu$  are very similar for each floor,  $\beta_{R,Ha}$  are almost the same along the height. Table 3.3 shows that  $\beta_{R,Ha}$  decreases as the  $P(D>C)_{50\text{ years}}$  increases. A



system with high  $R_\mu$  will have a low  $Sa_{y,exp}$  and high  $MAF(Sa > Sa_{y,exp})$ . Thus, from equation (11) we could indicate that a system with higher  $R_\mu$  needs a higher  $\beta_{R,Ha}$  to be considered as reliable as a system with a low  $R_\mu$  (Victorsson et al, 2016).

**Table 3. 3** The Reliability Index,  $\beta_{R,Ha}$

Story	$R_\mu$	$Sa_{y,exp}$	Long.=-117.818, Lat.=33.654				
			$P(D>C)_{50\ years}$				
			0.05%	0.10%	0.20%	0.50%	1.00%
6	3.7	0.2	2.8	2.5	2.3	1.9	1.6
5	3.7	0.2	2.8	2.5	2.3	1.9	1.6
4	3.7	0.2	2.8	2.5	2.3	1.9	1.6
3	3.8	0.2	2.8	2.5	2.3	1.9	1.6
2	3.8	0.2	2.8	2.6	2.3	1.9	1.6
1	3.8	0.2	2.8	2.6	2.3	1.9	1.6

The reliability index,  $\beta_{R,Ha}$ , in Table 3.3 are calculated by assuming the failures of force-controlled components always causes system collapse; the  $\Delta P(Coll_{D>C})_{50\ years} = P(D > C)_{50\ years}$ . The influence of capacity-designed component failure on the system collapse safety is investigated by adjusting  $P(Coll_{D>C}|D > C)$  equal to 0.75, 0.50, and 0.25 in equation (16) and comparing the  $\beta_{R,Ha}$  values. Figure 3.9 shows the reliability index at the 1<sup>st</sup> story of the system with different  $P(Coll_{D>C}|D > C)$  values. It is basically shows that, when the probability of the demand exceeding the capacity in the force-controlled component is less likely to cause collapse in the system, we can tolerate a lower reliability index. The previous assumption of  $P(Coll_{D>C}|D > C)$  used to calculate the values in Table 3.3 gives the most conservative result of reliability index.

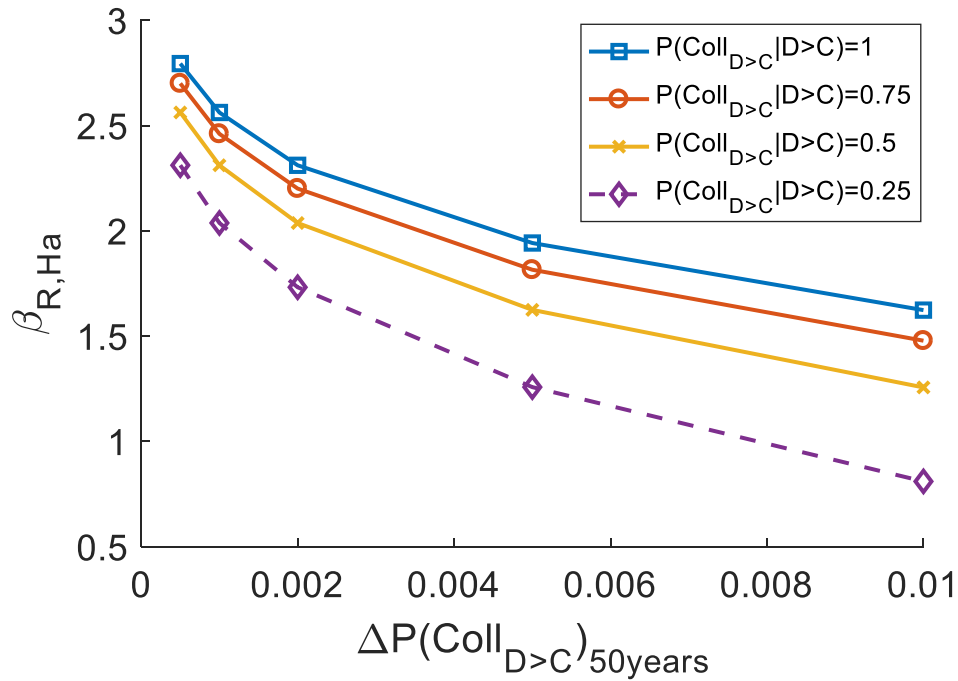


**Figure 3. 9** The Sensitivity of The Reliability Index,  $\beta_{R,Ha}$ , to the  $P(\text{Coll}_{D>C}|D > C)$

Once the analysis to determine the reliability index is completed, all the values needed to calculate the demand factors,  $\gamma$ , and capacity factors,  $\phi$ , of force-controlled components are available. Using the basic equation (9) and  $\rho = 0$  (assuming the demand and capacity in force-controlled components are uncorrelated), the capacity and demands factors for spine infill struts are calculated and shown in Table 3.4 to Table 3.8.

The capacity factors are determined by fixing the demand factors,  $\gamma$ , equal to 1.0. Note that the strength reduction factor is always taken to be less than or equal to one. If the value of  $\phi$  computed from equation (9) is greater than 1.0, a value of 1.0 is assigned. The 1<sup>st</sup> story, which has the largest ratio of  $\hat{D}_m/D_n$ , has the lowest capacity factors compared to the other stories. Therefore, the capacity and demand

factors at the 1<sup>st</sup> story will be used as the representative load and resistance factors for the force-controlled components. The tables also show that as the target probability of demand exceeding capacity in 50 years increases, the design of force-controlled components becomes more relaxed and the capacity factor increases. In other words, by adjusting a lower ratio of capacity and demands factor in design, the force-controlled component will have a lower likelihood to experience a force demand that is higher than its capacity.

**Table 3.4** Capacity and Demand Factors of Spine Infill Struts for 0.05% Probability of Demand Exceeding Capacity in 50 years

Story	$R_{\mu}$	$V_{y,exp}/V_{DBE}$	$Sa_{y,exp}$	$\beta_{R,Ha}$	$\phi/\gamma$	$\phi$	$\gamma$
6	3.7	1.6	0.2	2.8	0.9	0.9	1.00
5	3.7	1.6	0.2	2.8	0.6	0.6	1.00
4	3.7	1.6	0.2	2.8	0.7	0.7	1.00
3	3.8	1.6	0.2	2.8	0.7	0.7	1.00
2	3.8	1.6	0.2	2.8	0.6	0.6	1.00
1	3.8	1.6	0.2	2.8	0.2	0.2	1.00

**Table 3. 5** Capacity and Demand Factors of Spine Infill Struts for 0.1% Probability of Demand Exceeding Capacity in 50 years

Story	$R_{\mu}$	$V_{y,exp}/V_{DBE}$	$Sa_{y,exp}$	$\beta_{R,Ha}$	$\phi/\gamma$	$\phi$	$\gamma$
6	3.7	1.6	0.2	2.5	0.9	0.9	1.00
5	3.7	1.6	0.2	2.5	0.7	0.7	1.00
4	3.7	1.6	0.2	2.5	0.7	0.7	1.00
3	3.8	1.6	0.2	2.5	0.7	0.7	1.00
2	3.8	1.6	0.2	2.6	0.6	0.6	1.00
1	3.8	1.6	0.2	2.6	0.2	0.2	1.00

**Table 3. 6** Capacity and Demand Factors of Spine Infill Struts for 0.2% Probability of Demand Exceeding Capacity in 50 years

Story	$R_{\mu}$	$V_{y,exp}/V_{DBE}$	$Sa_{y,exp}$	$\beta_{R,Ha}$	$\phi/\gamma$	$\phi$	$\gamma$
6	3.7	1.6	0.2	2.3	1.0	1.0	1.00
5	3.7	1.6	0.2	2.3	0.7	0.7	1.00
4	3.7	1.6	0.2	2.3	0.8	0.8	1.00
3	3.8	1.6	0.2	2.3	0.8	0.8	1.00
2	3.8	1.6	0.2	2.3	0.6	0.6	1.00
1	3.8	1.6	0.2	2.3	0.2	0.2	1.00

**Table 3. 7** Capacity and Demand Factors of Spine Infill Struts for 0.5% Probability of Demand Exceeding Capacity in 50 years

Story	$R_{\mu}$	$V_{y,exp}/V_{DBE}$	$Sa_{y,exp}$	$\beta_{R,Ha}$	$\phi/\gamma$	$\phi$	$\gamma$
6	3.7	1.6	0.2	1.9	1.2	1.0	1.00
5	3.7	1.6	0.2	1.9	0.8	0.8	1.00
4	3.7	1.6	0.2	1.9	0.9	0.9	1.00
3	3.8	1.6	0.2	1.9	0.9	0.9	1.00
2	3.8	1.6	0.2	1.9	0.7	0.7	1.00
1	3.8	1.6	0.2	1.9	0.3	0.3	1.00

**Table 3. 8** Capacity and Demand Factors of Spine Infill Struts for 1% Probability of Demand Exceeding Capacity in 50 years

Story	$R_{\mu}$	$V_{y,exp}/V_{DBE}$	$Sa_{y,exp}$	$\beta_{R,Ha}$	$\phi/\gamma$	$\phi$	$\gamma$
6	3.7	1.6	0.2	1.6	1.3	1.0	1.00
5	3.7	1.6	0.2	1.6	0.8	0.8	1.00
4	3.7	1.6	0.2	1.6	0.9	0.9	1.00
3	3.8	1.6	0.2	1.6	0.8	0.8	1.00
2	3.8	1.6	0.2	1.6	0.7	0.7	1.00
1	3.8	1.6	0.2	1.6	0.2	0.2	1.00

The load and resistance factors presented in Table 3.4 to 3.8 are based on the assumption that there is no correlation between the capacity and demand,  $\rho = 0$ . In order to investigate the sensitivity of  $\phi/\gamma$  to the correlation of capacity and demand, the spine infill strut at the 1<sup>st</sup> story is assessed by applying  $\rho$  values equal to 0, 0.50, and 0.75 to equation (9).

For a target  $P(D > C)_{50\ years} = 0.1\ %$ , the result shows that  $\phi/\gamma$  increases with the  $\rho$  value. In other words, the most conservative result is obtained by assuming the probability of demand and the capacity are uncorrelated.

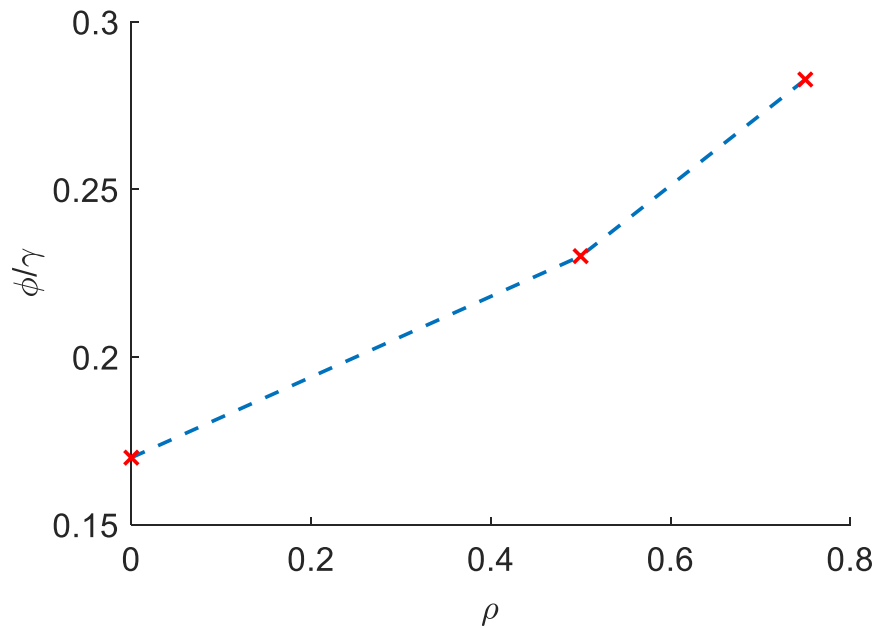


**Figure 3.10** The Sensitivity of  $\phi/\gamma$  to  $\rho$  Factor

Using the same steps as the spine infill struts, the capacity and demands factor of spine beams and columns are calculated. The results of capacity-based requirement for beams and columns with 0.1% target probability of demand exceeding capacity in 50 years are summarized in Table 3.8 and Table 3.9. The  $\phi/\gamma$  for columns and beams are significantly larger than spine infills struts. The results are expected since the normalized demands of spine infills struts at the 1<sup>st</sup> story (Figure 3.2) are exceeding 1.0, meanwhile the normalized demands in beams and columns at the 1<sup>st</sup> story (Figure 3.3 and 3.4, respectively) and columns are under 1.0.

**Table 3.9** Capacity and Demand Factors of Spine Beams for 0.1% Probability of Demand Exceeding Capacity in 50 years

Story	$R_{\mu}$	$V_{y,exp}/V_{RSA}$	$Sa_{y,exp}$	$\beta_{R,Ha}$	$\phi/\gamma$	$\phi$	$\gamma$
6	3.7	1.6	0.2	2.5	1.9	1.0	1.0
5	3.7	1.6	0.2	2.5	1.8	1.0	1.0
4	3.7	1.6	0.2	2.5	2.0	1.0	1.0
3	3.8	1.6	0.2	2.5	2.3	1.0	1.0
2	3.8	1.6	0.2	2.6	1.8	1.0	1.0
1	3.8	1.6	0.2	2.6	1.3	1.0	1.0

**Table 3.10** Capacity and Demand Factors of Spine Columns for 0.1% Probability of Demand Exceeding Capacity in 50 years

Story	$R_{\mu}$	$V_{y,exp}/V_{RSA}$	$Sa_{y,exp}$	$\beta_{R,Ha}$	$\phi/\gamma$	$\phi$	$\gamma$
6	3.7	1.6	0.2	2.5	6.3	1.0	1.0
5	3.7	1.6	0.2	2.5	7.2	1.0	1.0
4	3.7	1.6	0.2	2.5	7.2	1.0	1.0
3	3.8	1.6	0.2	2.5	6.7	1.0	1.0
2	3.8	1.6	0.2	2.6	3.4	1.0	1.0
1	3.8	1.6	0.2	2.6	1.3	1.0	1.0

## 4. CONCLUSIONS

A six-story concrete frame with a rocking spine system is analyzed using a reliability-based method (Victorsson et al. 2013) with the purpose of determining the load and resistance factors for its force-controlled components. The building design used in this study is from the work of Burton et al (2016). The system is modelled in OpenSees and analyzed using incremental dynamic analysis (IDA) to obtain the demand of the force-controlled component; spine-infill struts axial forces, spine-beam moments, and spine-column moments. The system is also modelled in ETABS and analyzed using Response Spectrum Analysis to determine the system's yield modification factor,  $R_\mu$  which useful for determining the intensity that initiates yielding in deformation-controlled components,  $Sa_{y,exp}$  and establishing the probability of the structure is subjected to the design forces.

The reliability index,  $\beta_{R,Ha}$ , is calculated from the mean annual frequency (MAF) of exceeding the ground motion intensity level defined by  $Sa_{y,exp}$ , and the MAF of the demand exceeding the capacity in force-controlled components. The  $\beta_{R,Ha}$ , depends on the site's ground motion hazard curve and the system (sub-system) yield modification factor,  $R_\mu$ , the tolerable added probability of collapse due to the failure of force-controlled components,  $\Delta P(\text{Coll}_{D>C})_{50 \text{ years}}$ , and the influence of the demand exceeding capacity on structural components to the system collapse,  $P(\text{Coll}_{D>C} | D > C)$ . The study finds that the reliability index increases with  $R_\mu$ . Systems or subsystems with lower  $R_\mu$  are stronger system and require larger shaking



intensities to induce yielding in deformation-controlled components. With the same target of added probability of collapse, a system with lower  $R_{\mu}$  will have a lower  $\beta_{R,H\alpha}$ .

In this study, five different  $\Delta P(\text{Coll}_{D>C})_{50 \text{ years}}$  are used; 0.05%, 0.1%, 0.20%, 0.50%, and 1%. By considering the collapse risk threshold of a modern code-conforming structures equal to 1% (ASCE 7-10),  $\Delta P(\text{Coll}_{D>C})_{50 \text{ years}}$  values will add the total collapse threshold to be 1.05%, 1.1%, 1.2%, 1.5%, and 2%, respectively. If the failure of force-controlled components assumed always causes system collapse,  $P(\text{Coll}_{D>C} | D > C) = 1$ , the values of  $\Delta P(\text{Coll}_{D>C})_{50 \text{ years}}$  is equal to the probability of demand exceeding capacity in 50 years,  $P(D > C)_{50 \text{ years}}$ . From the sensitivity analysis, this assumption gives the most conservative result of  $\beta_{R,H\alpha}$ .

Once the  $\beta_{R,H\alpha}$ , median and nominal demands and capacity are determined, the demand and capacity factors can be calculated. The results show that the 1<sup>st</sup> story has the most critical ratio of capacity,  $\phi$  and demand factors,  $\gamma$ .  $\phi/\gamma$  increases with the  $P(D > C)_{50 \text{ years}}$ . By setting the load factor,  $\gamma$ , equal to 1.0, the capacity factor,  $\phi$ , of spine infill struts, spine-beams, and spine-columns corresponding to 0.1% target  $P(D > C)_{50 \text{ years}}$  are 0.2, 1.0, and 1.0, respectively. The results show that if we want to avoid damages in spine infills at the MCE level intensity, we need to increase the strength of the struts by 5 times which is unrealistic. Thus, we would be expected and should tolerate some damage to the spine at the MCE level. Further studies are needed to determine how much damage is acceptable in the spine infills. Since the

spine beams were designed to be the same as the non-spine beams, even though the design loads are much lower, no resistance factor required. The same goes for the spine columns. Since the designed spine columns provide much higher axial and moment resistance than their demands, this force-controlled component is generally designed conservatively. The  $\phi/\gamma$  described before are based on the assumption that the probability of demand and capacity are uncorrelated,  $\rho = 0$ . The sensitivity analysis shows that as the  $\rho$  value increases, the  $\phi/\gamma$  also increases. The trend is consistent with equation (9).

The results of this study are still insufficient to be used to develop codes guidelines for rocking spine systems. More studies are needed in the future to determine the capacity-based design requirements for rocking spine force-controlled components. One of the issues that need to be addressed in the further studies is the effect of reliability index dependency to the hazard curve of the specified sites, i.e. a different location will have a different load and resistance factors. Beside of the cumbersome calculation, it is probably unrealistic to have different load factors for different sites. Victorsson (2013) partially addressed the issue by developing a simplified equation to determine the reliability index using the slope between two spectral intensities,  $S_a$ , and corresponding hazard levels,  $H_a$ . The equation was obtained from a regression linear analysis and has a coefficient of determination,  $R^2 = 0.96$ . The same approach can be applied to develop a similar empirical equation for rocking spine system, which can be used to exercise load and resistance factors for different seismic design categories (SDCs) by picking a set of characteristic sites consistent slope and hazard

level ranges for a given SDC. The values for building codes can be obtained from the most conservative set of factors for each SDC. Another issue is in this study the spine infill struts, spine beams, and spine columns are assumed to have the same ratio of the median and nominal capacity,  $\hat{C}_M/C_N$ , of. Data from actual tests might give more accurate results.

## REFERENCES

- ASCE. (2010). Minimum Design Loads For Buildings and Other Structures. In *ASCE 7-10*. Reston, VA.
- Burton, H. V., Deierlein, G. G., Mar, D., Mosalam, K. M., Rodgers, J., & Gunay, S. (2016). Rocking Spine for Enhanced Seismic Performance of Reinforced Concrete Frames with Infills. *Journal of Structural Engineering*. doi:10.1061/(ASCE)ST.1943-541X.0001574
- FEMA. (2009). Quantification of Building Seismic Performance Factors. In *FEMA P965*. Redwood City, CA: Applied Technology Council.
- Mosalam, K., & Gunay, S. (2010). Seismic Retrofit of Non-ductile Reinforced Concrete Frames Using Infill Walls as a Rocking Spine. *Advances in Performance-Based Earthquake Engineering*, 349-357.
- Saneinejad, A., & Hobbs, B. (1995). Inelastic Design of Infilled Frames. *Journal of Structural Engineering*, 634-650.
- Toranzo, L. A. (2001). Displacement Based Design of Rocking Walls Incorporating Hysteretic Energy Dissipators.
- Vamvatsikos, D., & Cornell, A. (2002). Incremental Dynamic Analysis. *Earthquake Engineering and Structural Dynamic*, 491-514. doi:10.1002/eqe.141
- Victorsson, K. V. (2013). *The Reliability of Capacity-Designed Components in Seismic Resistant Systems*. Dissertation. Stanford University.
- Victorsson, V. K., Baker, J. W., & Deierlien, G. G. (2014). Reliability Considerations in the Seismic Capacity Design Requirements For Force Controlled Components. (M. Fischinger, Ed.) *Performance-Based Seismic Engineering: Vision for an Earthquake Resilient Society, Geological and Earthquake Engineering* 32, 435-447. doi:10.1007/978-94-017-8875-5\_\_29